Radiology

# Apparent Diffusion Coefficient as an MR Imaging Biomarker of Low-Risk Ductal Carcinoma in Situ: A Pilot Study[1]

Mami Iima, MD
Denis Le Bihan, MD, PhD
Ryosuke Okumura, MD, PhD
Tomohisa Okada, MD, PhD
Koji Fujimoto, MD, PhD
Shotaro Kanao, MD
Shiro Tanaka, PhD
Masakazu Fujimoto, MD
Hiromi Sakashita, MD, PhD
Kaori Togashi, MD, PhD

**Purpose:** To evaluate the potential of apparent diffusion coefficients (ADCs) obtained at quantitative diffusion-weighted magnetic resonance (MR) imaging of the breast as a biomarker of low-grade ductal carcinoma in situ (DCIS).

**Materials and Methods:** This retrospective study was approved by an institutional review board, and the requirement to obtain informed consent was waived. Twenty-two women (age range, 36–75 years; mean age, 56.4 years) with pure DCIS (seven with low-grade DCIS, five with intermediate-grade DCIS, and seven with high-grade DCIS) and three with microinvasion underwent breast MR imaging at 1.5 T between January 2008 and November 2010. MR examinations included contrast material–enhanced (gadoteridol) T1-weighted imaging and diffusion-weighted MR imaging with *b* values of 0 and 1000 sec/mm$^2$. ADC maps were generated. The distributions of the ADCs in regions of interest covering the lesions were compared among the three grades by using linear mixed-model analysis, and the discriminatory power of the lesion minimum ADC was determined with receiver operating characteristic analysis.

**Results:** The mean ADC was $1.42 \times 10^{-3}$ mm$^2$/sec (95% confidence interval [CI]: $1.31 \times 10^{-3}$ mm$^2$/sec, $1.54 \times 10^{-3}$ mm$^2$/sec) for low-grade DCIS, $1.23 \times 10^{-3}$ mm$^2$/sec (95% CI: $1.10 \times 10^{-3}$ mm$^2$/sec, $1.36 \times 10^{-3}$ mm$^2$/sec) for intermediate-grade DCIS, $1.19 \times 10^{-3}$ mm$^2$/sec (95% CI: $1.08 \times 10^{-3}$ mm$^2$/sec, $1.30 \times 10^{-3}$ mm$^2$/sec) for high-grade DCIS, and $2.06 \times 10^{-3}$ mm$^2$/sec (95% CI: $1.94 \times 10^{-3}$ mm$^2$/sec, $2.18 \times 10^{-3}$ mm$^2$/sec) for normal breast tissue. The mean ADCs for high- and intermediate-grade DCIS were significantly lower than that for low-grade DCIS ($P < .01$ and $P = .03$, respectively), and the mean ADC for low-grade DCIS was significantly lower than that for normal tissue ($P < .001$). The lesion minimum ADC for low-grade DCIS was also significantly higher than that for high- and intermediate-grade DCIS ($P < .01$). A threshold of $1.30 \times 10^{-3}$ mm$^2$/sec for the minimum ADC in the diagnosis of low-grade DCIS had a specificity of 100% (12 of 12 patients; 95% CI: 73.5%, 100%) and a positive predictive value of 100% (four of four patients; 95% CI: 39.8%, 100%).

**Conclusion:** These preliminary results suggest that quantitative diffusion-weighted MR imaging could be used to identify patients with low-grade DCIS with very high specificity. If the results of this study are confirmed, this approach could potentially spare those patients from invasive approaches such as mastectomy or axillary lymph node excision.



[1] From the Department of Diagnostic Imaging and Nuclear Medicine (M.I., T.O., K.F., S.K., K.T.) and Human Brain Research Center (D.L.B.), Kyoto University Graduate School of Medicine, 54 Shogoin Kawaharacho, Sakyoku, Kyoto 606-8507, Japan; Departments of Radiology (M.I., R.O.) and Pathology (M.F., H.S.), Kitano Hospital, Osaka, Japan; Neurospin, CEA-Saclay, Gif-sur-Yvette, France (D.L.B.); and Translational Research Center, Kyoto University Hospital, Kyoto, Japan (S.T.). Received October 7, 2010; revision requested November 22; revision received February 1, 2011; accepted March 16; final version accepted April 20. **Address correspondence to** M.I. (e-mail: *mamiiima@kuhp.kyoto-u.ac.jp*).

With the advent of widespread mammographic screening for breast cancer in the early to mid-1980s, the detection of ductal carcinoma in situ (DCIS) has increased worldwide. Currently, DCIS accounts for 20%–30% of all newly diagnosed breast cancers in the United States and approximately 20% of cases detected with mammography (1). An important issue, however, is that one cannot predict whether DCIS will evolve to invasive ductal carcinoma. Hence, even though low-grade DCIS may be considered a nonlethal type of tumor, all cases of DCIS are usually treated as though they will become invasive ductal carcinoma. Indeed, recent studies have pointed out that the natural history of low-grade DCIS can extend more than 4 decades and that it is unlikely to become invasive (2,3).

Recent immunohistochemical studies have revealed that, unlike adenoma-carcinoma of the colon, which evolves following a single line, benign proliferative breast disease, some low-grade DCIS, most high-grade DCIS, and invasive carcinoma develop through distinct pathways (4). Those findings suggest that different therapeutic approaches could be proposed according to DCIS grade. Hence, there is a need for more accurate DCIS grading at the time of the initial diagnosis to customize the therapeutic approach. With mammography, it is possible to suspect the presence of high-grade lesions on the basis of the morphologic characteristics of microcalcifications (5); however, grading of DCIS remains difficult, with sparse biopsy sampling, because high- and low-grade components may coexist in a patient or even within one duct.

Lately, breast magnetic resonance (MR) imaging has been successfully introduced in the management of breast cancer—particularly DCIS (6). Although mammography can depict 80%–85% of all DCIS, the sensitivity of MR imaging in the accurate assessment of the extent of DCIS reaches 89%, which is much higher than that of either mammography or ultrasonography (US) (55% and 47%, respectively) (7). There is increasing evidence to suggest that, overall, breast MR imaging may be more sensitive than mammography—especially in the diagnosis of high-grade DCIS (8,9).

More recently, diffusion-weighted MR imaging has been introduced for cancer imaging. Diffusion-weighted imaging is highly sensitive to tissue microstructure (10,11), and it has been observed that the apparent diffusion coefficient (ADC) is significantly reduced in primary or secondary cancer tissues (12–14)—although the exact mechanism between diffusion reduction and cell proliferation remains unclear (15). Diffusion-weighted imaging was found to have a very high sensitivity of 97% in the detection of breast malignancy (16). Diffusion-weighted images and quantitative ADC maps have been successfully used to differentiate between benign and malignant breast lesions as well as to depict tumor extension (17–19) and may have the potential to depict many mammographically and clinically occult breast carcinomas (20). In light of those encouraging results, we performed this study to evaluate the potential of ADCs obtained at quantitative diffusion-weighted MR imaging of the breast as a biomarker of low-grade DCIS.

### Advances in Knowledge

- The apparent diffusion coefficients (ADCs) of high- and intermediate-grade ductal carcinoma in situ (DCIS) lesions were significantly lower than those of low-grade DCIS ($P < .01$, $P = .03$, respectively), and there was a significant negative trend between mean ADC and tumor grade ($P < .01$).
- With use of receiver operating characteristic analysis, a cutoff value for the lesion minimum ADC was established under the restriction of 100% specificity (95% confidence interval: 73.5%, 100%) while maximizing sensitivity; all four patients whose minimum ADCs were above a threshold of $1.30 \times 10^{-3}$ mm$^2$/sec had low-grade DCIS.

### Implication for Patient Care

- Our preliminary results suggest that quantitative diffusion-weighted MR imaging could be used to identify patients with low-grade, low-risk DCIS with very high specificity and, if the results are confirmed, has the potential to spare patients from invasive approaches (eg, mastectomy or axillary lymph node excision); in addition, this approach could potentially decrease the anxiety of women diagnosed with low-risk DCIS by reassuring them of the noninvasive nature of the lesions.

## Materials and Methods

### Patients

Institutional review board approval was obtained, and the requirement to obtain informed consent was waived owing to the retrospective nature of this study. This study was a retrospective review of images from 25 women in whom DCIS was diagnosed after biopsy at Kitano Hospital between January 2008 and November 2010. DCIS was first suspected after patients underwent physical examination, mammography, and US. MR

**Published online before print**
10.1148/radiol.11101892 **Content codes:** BR OI BQ

**Radiology 2011;** 260:364–372

**Abbreviations:**
ADC = apparent diffusion coefficient
CI = confidence interval
DCIS = ductal carcinoma in situ
ROC = receiver operating characteristic
ROI = region of interest

**Author contributions:**
Guarantors of integrity of entire study, M.I., D.L.B., K.T.; study concepts/study design or data acquisition or data analysis/interpretation, all authors; manuscript drafting or manuscript revision for important intellectual content, all authors; approval of final version of submitted manuscript, all authors; literature research, M.I., D.L.B., R.O., T.O., S.T., K.T.; clinical studies, M.I., R.O., S.K., S.T., M.F., H.S., K.T.; experimental studies, D.L.B., K.T.; statistical analysis, D.L.B., K.F., K.T.; and manuscript editing, M.I., D.L.B., T.O., K.F., S.K., K.T.

Potential conflicts of interest are listed at the end of this article.

imaging was performed before or 2 weeks after biopsy to avoid artifacts. Mammography showed microcalcifications in 17 of the 25 patients and focal asymmetry suspicious for malignancy in five. There were no suspicious findings at mammography in three patients; however, two of the three patients were suspected of having DCIS at breast US and one patient had nipple erosion. Only patients with pure DCIS (without microinvasion or invasive breast cancer elsewhere) were enrolled in this study. Three patients were excluded from the study. Two patients (one with intermediate DCIS and one with low-to-intermediate-grade DCIS) were excluded because their diffusion-weighted images showed no contrast with the background owing to a very low signal-to-noise ratio, and one patient (with intermediate DCIS) was excluded because of incomplete fat suppression. Hence, 22 patients (age range: 36–75 years; mean age, 56.4 years) were initially included in this study. Seven patients had low-grade DCIS, five had intermediate-grade DCIS, seven had high-grade DCIS, and three had DCIS with microinvasion. One patient had a low-to-intermediate-grade DCIS, which was considered low-grade DCIS because the lesion was classified as Van Nuys Prognostic Index 4, which is associated with the best DCIS prognosis (21,22). Because the status of DCIS lesions with microinvasion is still controversial (23), the three patients with microinvasion were excluded from the statistical analysis performed only with pure DCIS cases.

### MR Image Acquisition

Breast MR imaging was performed by using a 1.5-T unit (Intera and Achieva; Philips Healthcare, Eindhoven, the Netherlands) equipped with a dedicated four-channel breast array coil. The following images were acquired after obtaining localizer images: bilateral sagittal fat-suppressed T2-weighted images (4937/90 [repetition time msec/echo time msec], 20-cm field of view, 256 × 256 matrix, 4-mm-thick sections, 162-second acquisition time); fat-suppressed, diffusion-weighted echo-planar images (8000/96; 40-cm field of view; 128 × 104 matrix interpolated to 256 × 256 [ie, 1.56 × 1.56-mm resolution]; parallel acquisition factor of 2; 5-mm-thick sections; 182-second acquisition time; and application of motion probing gradient pulses along the x, y, and z directions with $b$ values of 0 and 1000 sec/mm$^2$); and free-breathing dynamic contrast material–enhanced MR images, which were obtained by using a three-dimensional fat-suppressed T1-weighted gradient-echo sequence (6.1/3.5, 15° flip angle, 40-cm field of view, 400 × 400 matrix, 2-mm-thick sections reconstructed to 0.78 × 0.78 × 1-mm resolution, 255-second acquisition time), which were acquired before and immediately after infusion of 0.2 mL/kg gadoteridol (ProHance; Bracco-Eisai, Tokyo, Japan). Central k-space data were acquired first to catch early contrast enhancement. T1-weighted images were also acquired 9 minutes after infusion, but those images were not considered in this study. With diffusion-weighted imaging data, the quantitative diffusion (ADC) was calculated on a voxel-by-voxel basis as follows: ADC = $(1/b) \times \ln (S_0/S)$, where $S_0$ and $S$ are the signal intensities of each voxel obtained with values of 0 and 1000 sec/mm$^2$, respectively.

### Data Postprocessing

Two independent readers (M.I. [radiologist A] and R.O. [radiologist B], with 3 and 6 years of experience in breast MR imaging, respectively) manually drew regions of interest (ROIs) on the diffusion-weighted images ($b$ = 1000 sec/mm$^2$) (Figs 1, 2). The readers were blinded to the final pathologic results. ROIs were placed in regions with high signal intensity on the diffusion-weighted images; the contrast and morphologic characteristics at the early phase of contrast-enhanced T1-weighted imaging and T2-weighted imaging were used to guide ROI placement to avoid areas of T2 shine-through that are usually found in necrotic or cystic parts. The signal intensity of the lesion on the diffusion-weighted images was visually classified as high or low compared with that of the corresponding background breast tissue. T1-weighted images were also used retrospectively to assess the nature of borderline lesions with very high or very low ADCs. ROIs were defined as slightly smaller than the actual lesions to reduce partial volume effects, but only ROIs larger than 20 mm$^2$ were considered as meaningful and retained for further analysis. Because DCIS is usually a multifocal disease, several ROIs were drawn to depict each lesion. Hence, the number of ROIs for each patient varied from one to eight (Fig 3). Control ROIs were drawn in the normal homogeneous breast parenchyma in the center of the contralateral breast, avoiding contamination by fatty tissue. The average of mean ROI sizes of normal tissues was 140.1 mm$^2$ (range, 106.8–175.0 mm$^2$). The ROIs were then copied and pasted onto the corresponding ADC map for quantitative analysis. For each ROI, we extracted the mean ADC and the ROI area. The total lesion size, which was defined as the sum of the areas of all ROIs used to depict the lesion for each patient, was also compared among each grade. Because the scope of this study was purely focused on quantitative diffusion-weighted MR imaging, the kinetics of contrast enhancement were not considered. The value of contrast-enhanced MR imaging for DCIS has been reported elsewhere (8,24).

### Histopathologic Analysis

Histopathologic analysis was performed with use of specimens obtained from surgery (mastectomy or lumpectomy). Blocks were processed, and sections were cut and stained with hematoxylin and eosin according to standard pathology protocols and studied by experienced pathologists (H.S. and M.F., with 10 and 5 years of experience in breast pathology, respectively). Histologic circumscription without irregular, infiltrative, or fingerlike extensions into the adjacent stroma was regarded as indicative of a noninvasive growth pattern. Nuclear grade and presence of necrosis were assessed and the DCIS grade was established (25). On slides where microinvasion was suspected, immunohistochemistry was performed by using an automated immunostainer (Ventana BenchMark AutoStainer; Ventana Medical

**Figure 1**

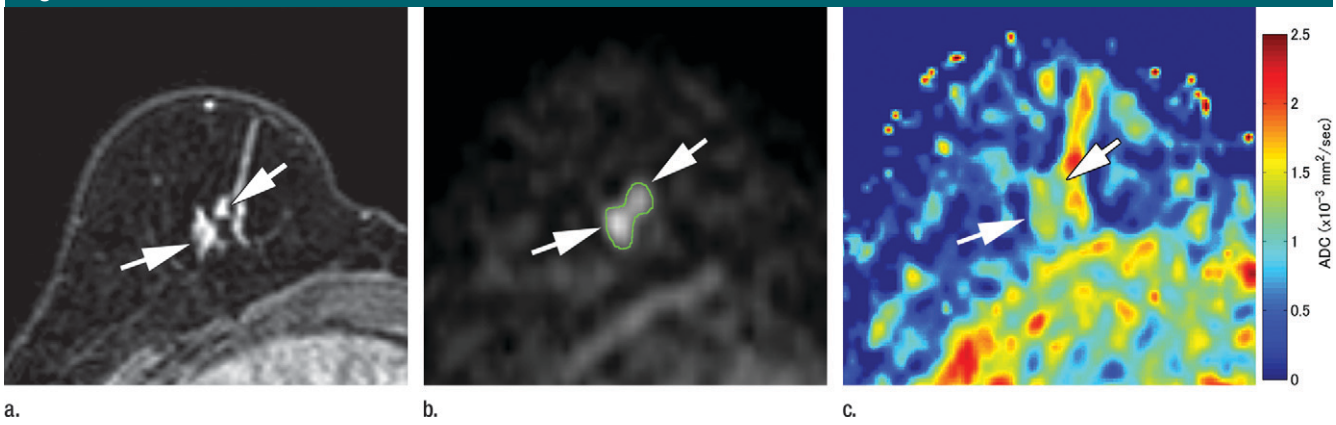


**Figure 1:** High-grade DCIS in a 56-year-old woman. **(a)** Dynamic contrast-enhanced MR image obtained in early phase, **(b)** diffusion-weighted MR image ($b$ = 1000 sec/mm$^2$), and **(c)** ADC map. **(a)** Areas of homogeneous nonmasslike enhancement (arrows) are shown; this image was used to identify lesions and define corresponding ROIs on **b** (arrows), where lesions are visible as areas of high signal intensity. **(c)** Lesion exhibits areas with light blue contours (arrows), which are indicative of low ADC.

**Figure 2**

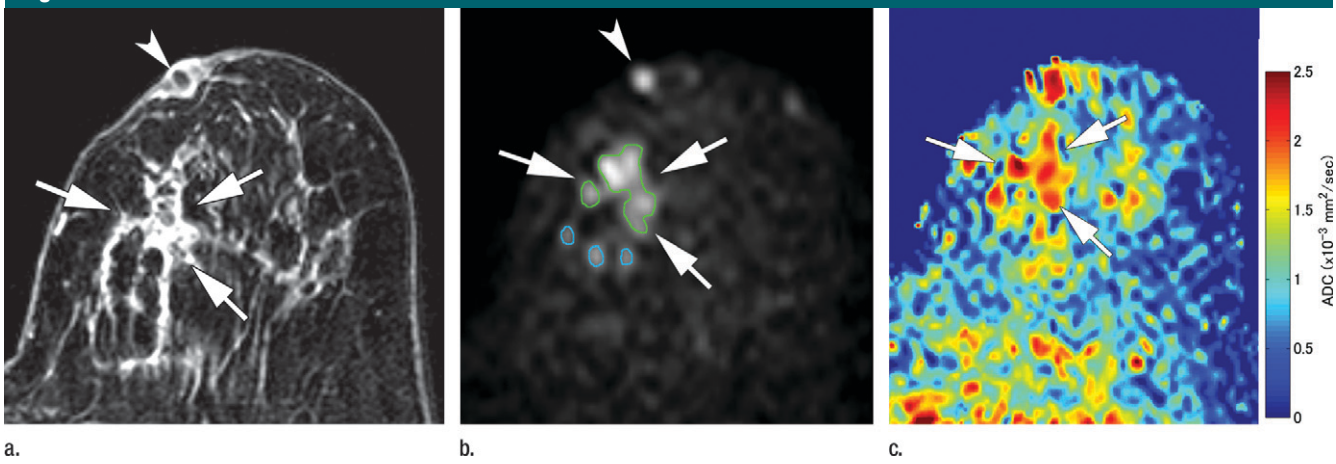


**Figure 2:** Low-grade DCIS (arrows) in a 68-year-old woman. **(a)** Dynamic contrast-enhanced MR image obtained in early phase, **(b)** diffusion-weighted MR image ($b$ = 1000 sec/mm$^2$), and **(c)** ADC map. In **c**, lesion has orange-red contours (corresponding to high ADC). In **b**, only ROIs outlined in green were analyzed; blue ROIs were excluded because they were smaller than 20 mm$^2$. The area of high signal intensity (arrowhead) on **b** was not outlined because it did not enhance on contrast-enhanced image (arrowhead). This area turned out to be nipple discharge.

Systems, Tucson, Ariz) with antibodies against two myoepithelial markers, CD10 (diluted 1:50; 56C6, Novocastra, Newcastle, United Kingdom) and p63 (diluted 1:25; 7JUL, Novocastra). Immunoreactivity for CD10 and p63 was evaluated at the periphery of each circumscribed nest, and lesions lacking immunoreactivity for myoepithelial markers were diagnosed as microinvasion.

### Statistical Analysis

To assess the reliability of our multiple ROI approach, the interobserver variability between radiologists A and B was evaluated by using intraclass correlation coefficient type "2,1" and the Pearson correlation coefficient for the mean ADC in the ROI and ROI size. The level of correlation was defined as very strong if $r$ = 1.0–0.9, strong if $r$ = 0.9–0.7, moderate if $r$ = 0.7–0.5, and weak if $r$ = <0.5. Then, ROIs from both radiologists were merged, taking the average value for the mean ADC and ROI size analyses.

To evaluate whether distributions of ADCs and ROI sizes differed among the three grades, "ROI-based" analysis was performed by using the mean ADC and the ROI sizes of all ROIs. We used linear mixed-model analysis for repeated measurement data (26) and estimated the least-square means (adjusted means) and the 95% confidence intervals (CIs) of the ADCs and ROI sizes in each grade adjusted for within-patient correlation. The $P$ values for the differences between low-grade DCIS and intermediate- or high-grade DCIS were adjusted for multiple comparisons with use of the Hochberg procedure. A $P$ value from a

Radiology

**Figure 3**

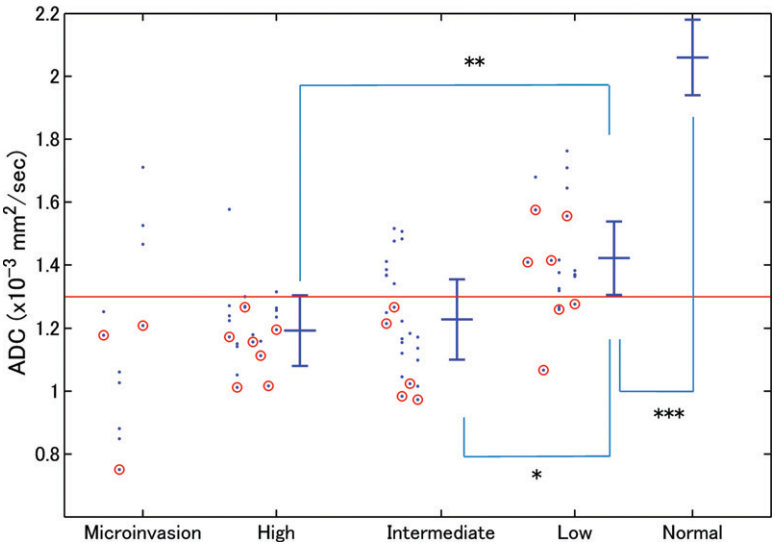


**Figure 3:** Graph shows distribution of ADCs for all ROIs. The mean ADC for each ROI (all 22 patients) is plotted, with data from each patient given in vertical columns. The number of ROIs per patient varied from one to eight. Patients are grouped according to lesion grade. Red circles = minimum ADC for each patient. The adjusted mean ADC and its 95% CI are shown for each grade as a vertical line to the right of each grade. The vertical line on right side of graph = mean ADC and 95% CI for normal breast tissue. The red line = ADC threshold of $1.30 \times 10^{-3}$ mm$^2$/sec for diagnosis of low-grade DCIS. All four patients whose minimum ADC was above this line had low-grade DCIS. * = $P < .05$ for comparison of intermediate- and low-grade DCIS, ** = $P < .01$ for comparison of high- and low-grade DCIS, and *** = $P < .001$ for comparison of low-grade DCIS and normal tissue. (ADC values for the three patients with microinvasion are shown for completeness, although they were excluded from statistical analysis.)

trend test was also calculated by using linear mixed models. The sample mean ADC of the low-grade DCIS lesions was compared with that of the normal breast tissue with a paired *t* test. Total lesion sizes for all patients across low, intermediate, and high grades were compared by using linear model analysis by estimating their sample means and their 95% CIs in each grade.

After establishing a statistically significant (negative) correlation between tumor grade and ADC, we tried to define a "patient-based" diagnostic procedure to identify low-grade lesions with the highest specificity. We hypothesized that the potentially most active part of the lesion is associated with the lowest ADC, and we investigated the diagnostic value of the lesion minimum ADC (defined as the ADC of the ROI with the lowest ADC within the lesion) for each patient. The minimum ADCs across low, intermediate, and high grades were first compared by estimating the sample means and the 95% CIs in each grade. *P* values for the differences between low-grade DCIS and intermediate- or high-grade DCIS were adjusted for multiple comparisons by using the Hochberg procedure. A *P* value from a trend test was also calculated by using general linear models.

The effectiveness of this diagnostic procedure in the differentiation of low-grade DCIS from non-low-grade DCIS was evaluated by using receiver operating characteristic (ROC) analysis. With use of ROC analysis, a cutoff value for the lesion minimum ADC was established under the restriction of 100% specificity while maximizing sensitivity.

For the ROI and lesion size statistical analysis, a log transformation was used to account for the skewness of the distribution. For all tests, $P < .05$ was considered indicative of a statistically significant difference. All statistical analyses was conducted by using software (Medcalc, version 11.3.2.0 [MedCalc Software, Mariakerke, Belgium], and SAS, version 9.2 [SAS Institute, Cary, NC]).

## Results

### MR Imaging Findings

The typical appearance of high- and low-grade tumors on contrast-enhanced T1-weighted images, diffusion-weighted images ($b$ = 1000 sec/mm$^2$), and ADC maps is shown in Figures 1 and 2. Two cases of low-grade DCIS exhibited low contrast, whereas all other lesions showed high contrast with surrounding tissue on diffusion-weighted images ($b$ = 1000 sec/mm$^2$). Results from all patients are summarized in Figure 3.

Some low-grade DCIS lesions contained parts with very low ADCs—even lower than those of high-grade DCIS. In one patient, the minimum ADC was $1.07 \times 10^{-3}$ mm$^2$/sec; this was probably related to bleeding or high protein content, as suspected from very high signal intensities on the T1-weighted images. Another patient with a high-grade lesion had one region with a very high ADC ($1.58 \times 10^{-3}$ mm$^2$/sec). The lesion was situated very near the nipple, and a collection of mucous or liquid due to the obstruction of the duct by the lesion may have resulted in the high ADC.

### Interobserver Variability

Radiologist A identified 69 ROIs (24 for high-grade DCIS, 24 for intermediate-grade DCIS, and 21 for low-grade DCIS), and radiologist B identified 66 ROIs (22 for high-grade DCIS, 24 for intermediate-grade DCIS, and 20 for low-grade DCIS). The Pearson correlation of the 66 ROIs was strong (0.91 for mean ADC, 0.95 for ROI size), and the intraclass correlation of the 66 ROIs was moderate (0.72 for mean ADC, 0.56 for ROI size). It is important to note that the lesion minimum ADC (see below) was not found in the three ROIs identified by radiologist A and not by radiologist B.

### Comparison of ADCs across Grades

The adjusted mean ADC of all ROIs was $1.42 \times 10^{-3}$ mm$^2$/sec (95% CI: $1.31 \times 10^{-3}$ mm$^2$/sec, $1.54 \times 10^{-3}$ mm$^2$/sec) for low-grade DCIS, $1.23 \times 10^{-3}$ mm$^2$/sec (95% CI: $1.10 \times 10^{-3}$ mm$^2$/sec, $1.36 \times 10^{-3}$ mm$^2$/sec) for intermediate-grade DCIS, and $1.19 \times 10^{-3}$ mm$^2$/sec (95% CI: $1.08 \times 10^{-3}$ mm$^2$/sec, $1.30 \times 10^{-3}$ mm$^2$/sec) for high-grade DCIS (Table 1). The mean ADC of high-grade DCIS lesions was significantly lower than that of low-grade DCIS lesions ($P < .01$). The mean ADC of intermediate-grade DCIS was also significantly lower than that of low-grade DCIS ($P = .03$), and there was a significant negative trend between mean ADC and lesion grade ($P < .01$) despite the overlap between ADCs. The sample mean in normal tissue was $2.06 \times 10^{-3}$ mm$^2$/sec (range, 1.32–2.47 $\times 10^{-3}$ mm$^2$/sec; 95% CI: $1.94 \times 10^{-3}$ mm$^2$/sec, $2.18 \times 10^{-3}$ mm$^2$/sec). The mean ADC of low-grade DCIS was significantly lower than that of normal breast tissues ($P < .001$).

The mean minimum ADC was $1.35 \times 10^{-3}$ mm$^2$/sec (95% CI: $1.24 \times 10^{-3}$ mm$^2$/sec, $1.46 \times 10^{-3}$ mm$^2$/sec) for low-grade DCIS, $1.09 \times 10^{-3}$ mm$^2$/sec (95% CI: $0.97 \times 10^{-3}$ mm$^2$/sec, $1.22 \times 10^{-3}$ mm$^2$/sec) for intermediate-grade DCIS, and $1.11 \times 10^{-3}$ mm$^2$/sec (95% CI: $1.01 \times 10^{-3}$ mm$^2$/sec, $1.22 \times 10^{-3}$ mm$^2$/sec) for high grade DCIS (Table 2). The minimum ADC of low-grade DCIS was significantly higher than that of high-grade DCIS ($P < .01$). The minimum ADC of intermediate-grade DCIS was significantly different from that of low-grade DCIS ($P < .01$). There was a significant negative trend between minimum ADC and lesion grade ($P < .01$). The minimum ADCs for the three lesions with microinvasion were 0.75, 1.18, and $1.21 \times 10^{-3}$ mm$^2$/sec.

### Comparison of ROI and Lesion Sizes across Grades

The adjusted means of the ROI sizes were 65.2 mm$^2$ (95% CI: 42.8 mm$^2$, 99.1 mm$^2$), 88.1 mm$^2$ (95% CI: 56.4 mm$^2$, 138.7 mm$^2$), and 45.2 mm$^2$ (95% CI: 30.2 mm$^2$, 67.6 mm$^2$) for low-, intermediate-, and high-grade DCIS, respectively (Table 3). The difference in ROI size between high- and low-grade lesions was not significant ($P = .21$), and there was not a significant negative trend between ROI size and tumor grade ($P = .25$). The sample means of the total lesion sizes were 303.6 mm$^2$ (95% CI: 91.4 mm$^2$, 515.7 mm$^2$), 521.0 mm$^2$ (95% CI: 270.0 mm$^2$, 772.0 mm$^2$), and 165.7 mm$^2$ (95% CI: 46.4 mm$^2$, 377.9 mm$^2$) for low-, intermediate-, and high-grade DCIS, respectively. There was also no statistically significant difference in the total lesion size among grades ($P = .39$). It should be noted that, although the total lesion size reflects the real lesion size, it is actually slightly smaller because only ROIs with a surface larger than 20 mm$^2$ were considered.

**Table 1**

**ROI-Level Comparison of Mean ADCs across Pathologic Grades**

| | ADC ($\times 10^{-3}$ mm$^2$/sec) | | | | |
|---|---|---|---|---|---|
| Grade | Adjusted Mean | Median | Range | 95% CI | *P* Value* |
| Low | 1.42 | 1.41 | 1.07–1.76 | 1.31, 1.54 | Ref |
| Intermediate | 1.23 | 1.12 | 0.97–1.52 | 1.10, 1.36 | .03 |
| High | 1.19 | 1.23 | 1.01–1.58 | 1.08, 1.30 | <.01 |

Note.—Results of a trend test showed a significant negative trend between mean ADC and lesion grade ($P < .01$, linear mixed model) despite the overlap between ADCs.

* *P* values reflect the difference in mean ADC from low-grade DCIS. All *P* values were significant after adjustment for multiplicity with the Hochberg procedure. Ref = reference.

**Table 2**

**Patient-Level Comparison of Minimum ADCs across Pathologic Grades**

| | ADC ($\times 10^{-3}$ mm$^2$/sec) | | | |
|---|---|---|---|---|
| Grade | Sample Mean | Range | 95% CI | *P* Value* |
| Low | 1.35 | 1.07–1.55 | 1.24, 1.46 | Ref |
| Intermediate | 1.09 | 0.98–1.26 | 0.97, 1.22 | <.01 |
| High | 1.11 | 1.00–1.26 | 1.01, 1.22 | <.01 |

Note.—Results of a trend test showed a significant negative trend between mean ADC and lesion grade ($P < .01$, linear mixed model) despite the overlap between ADCs.

* *P* values reflect the difference in mean ADC from low-grade DCIS. All *P* values were significant after adjustment for multiplicity with the Hochberg procedure. Ref = reference.

### ROC Curve Analysis

The discriminatory power of the lesion minimum ADC (to differentiate low-grade DCIS from non-low-grade DCIS) was good, with an area under the ROC curve of 0.89 (95% CI: 0.66, 0.99) for radiologist A and 0.88 (95% CI: 0.65, 0.98) for radiologist B (Fig 4).

The minimum ADC to obtain 100% specificity (12 of 12 patients; 95% CI: 73.5%, 100%) while maximizing sensitivity was $1.30 \times 10^{-3}$ mm$^2$/sec. All four patients whose minimum ADC was above this threshold had low-grade DCIS. On the basis of this threshold, the same four of 19 patients (21%) would have been correctly identified by each of the two radiologists as having low-grade DCIS with a positive predictive value of 100% (four of four patients; 95% CI: 39.8%, 100%) and a specificity of 100% (12 of 12 patients; 95% CI: 73.5%, 100%). None of the patients with intermediate- or high-grade DCIS or microinvasion had a minimum ADC below the threshold. The sensitivity was 57% (four of seven patients; 95% CI: 18.4%, 90.1%), and the negative predictive value was 80% (12 of 15 patients; 95% CI: 51.9%, 95.7%).

## Discussion

The diagnosis of DCIS is rapidly increasing because of the widespread use of

**Table 3**

**ROI-Level Comparison of Mean ROI Sizes according to Pathologic Grade**

| | ROI Size ($mm^2$) | | | | |
|---|---|---|---|---|---|
| Grade | Adjusted Mean* | Median | Range | 95% CI | *P* Value† |
| Low | 65.2 | 63.5 | 24.5–272.0 | 42.8, 99.1 | Ref |
| Intermediate | 88.1 | 96.3 | 35.5–334.5 | 56.4, 138.7 | .32 |
| High | 45.2 | 42.5 | 24.5–144.5 | 30.2, 67.6 | .21 |

Note.—Results of a trend test did not show a significant negative trend between ROI size and tumor grade (*P* = .25, linear mixed model).

* A log transformation was used to account for the skewness of the distribution on the histogram. Adjusted means were converted back with an inverse transformation.

† *P* values reflect the difference in mean ROI size from low-grade DCIS. Ref = reference.

**Figure 4**

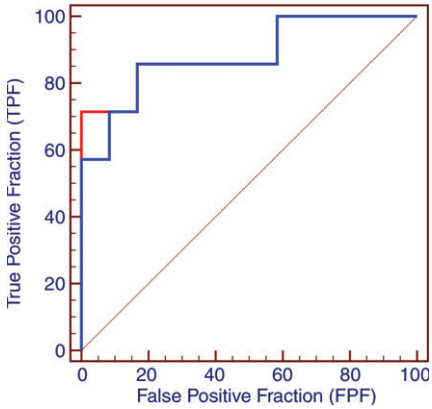


**Figure 4:** Graph shows ROC curves for differentiating low-grade DCIS from other grades of DCIS on the basis of minimum ADC values. Red line = radiologist A, blue line = radiologist B. The area under the ROC curve was 0.89 (95% CI: 0.66, 0.99) for radiologist A and 0.88 (95% CI: 0.65, 0.98) for radiologist B. Diagonal reference line indicates worst discriminatory power.

screening mammography. Even though DCIS lesions usually do not become invasive, patients in whom DCIS is diagnosed are usually treated as though they will have invasive carcinoma. The social, ethical, and economic consequences of such management are huge: More than 40% of women with DCIS undergo mastectomy, at a rate of some 10000 per year (1). Clearly one should look for new biomarkers to better predict the grade and outcome of diagnosed DCIS (27) and decrease the costly, and potentially unnecessary, use of extensive surgery (eg, mastectomy or axillary lymph node excision)—the morbidity of which is not negligible (28,29). It would also reduce surgical scars, which might mimic lesions on subsequent MR images. In our pilot study, we found a significant negative correlation between ADC and DCIS grade. Furthermore, an ADC threshold was established to help identify low-grade DCIS lesions with very high specificity. In the future, the ADC could well become such a biomarker.

Contrast-enhanced MR imaging has been proposed in the grading of active tumors (8). However, it only reflects the tumor vascular bed and provides no information about tumor cellularity, which is important for determining tumor grade. The ADC has been shown to correlate with cellular density in breast cancer (17). We hypothesize that the increase in membrane density that accompanies active cell proliferation hinders water diffusion, resulting in a decrease in ADC (15). High-grade lesions with the highest cell proliferation rate would have the lowest ADCs, as in brain tumors (30,31). In breast tumors, however, this correlation between tumor cellularity and ADC is still controversial (17,32). Although it is considered that a DCIS tumor size of more than 2.5 cm has a higher risk of microinvasion or invasion (33), we did not find any correlation among overall lesion size, grade, and ADC, in accordance with a previous study (34).

Because of the multifocal nature of DCIS lesions, we based our first analysis on the use of all individual ROIs, an important step in depicting nonmass lesions, as several grades might be present at the same time. The statistical significance of the negative correlation found between tumor grade and ADC, as seen in invasive ductal carcinoma (17,19), suggests that the most malignant part of a tumor is associated with the ROI with the lowest ADC. Indeed, the concept of "minimum ADC" is central because, as shown in the spectrum of values seen in some of our patients, the values can vary. It is important to consider that although there are, of course, overlaps in the ADCs for the high-, intermediate-, and low-grade lesions in the patient population, it is apparently possible to establish a minimum ADC threshold of potential clinical importance with which to identify low-grade lesions.

The use of ROIs is much more robust and less sensitive to noise than is the use of voxel minimum ADC values that have sometimes been used (31,35). Approximately 4%–23% of biopsied DCIS lesions will eventually prove to be invasive breast cancer at final pathologic examination (36,37). Although the sensitivity of open excisional biopsy reaches almost 100%, it is not applied to all DCIS cases because of its invasiveness. One may argue that diffusion-weighted imaging does not have the resolution to depict invasiveness at a microscopic level compared with biopsy, but biopsy sampling is necessarily sparse and the possibility of scrutinizing the whole lesion with diffusion-weighted imaging, especially when different grades might coexist, may outbalance this limitation.

Most diffusion-weighted imaging studies of the breast have been performed at 1.5 T, with a wide range of *b* values (34,38,39), but ADC accuracy improves with *b* values of more than 850 $sec/mm^2$ at 3.0 T (40). Our choice of *b* values as high as 1000 $sec/mm^2$ was motivated by the low ADCs found in high-grade lesions, ADCs that are close to those in the brain. With large *b* values, lesions with low ADC appear with a much better contrast. This is especially useful in high-density breasts, where MR imaging appears to be better than mammography (41), and the prevalence of DCIS seems to be slightly higher for young women with high-density breasts (42).

A limitation of our study is the small population size; our minimum ADC threshold value might not be representative of that of a larger population, including patients with lesions other than DCIS. Because the ADC is also reduced in other breast malignancies (17,19), our minimum ADC concept could probably be extended to non-DCIS lesions pending further investigation with a larger patient cohort. Identification of lesions on diffusion-weighted images may not always be easy. Artifacts such as susceptibility, chemical shift, or distortion, for which diffusion-weighted echo-planar imaging is very sensitive, could impair ADC measurements (43). T2 shine-through and blackout effects, hemorrhage, necrosis, cystic lesions, or mucous protein components may cause changes in signal intensity on diffusion-weighted images. It is important to emphasize the need for high-quality diffusion-weighted images and fat suppression to achieve reliable quantitative diffusion MR images. Fat exhibits very low ADCs and may mimic high-grade lesions. Conversely, efficient fat suppression may also interfere with ADC measurements when fatty and tumor tissues overlap, possibly decreasing the signal intensity level substantially. It is always a good practice to check the overall signal intensity level before assessing borderline ADCs.

In summary, we found a negative correlation between ADC and DCIS grade. In addition, we determined an ADC threshold ($1.3 \times 10^{-3}$ $mm^2$/sec) that can help identify low-grade DCIS lesions with high specificity. Although further prospective assessment in a larger patient cohort is needed, the results of our study suggest that ADCs obtained with quantitative diffusion-weighted MR imaging may play a role as a highly specific biomarker for low-grade DCIS. Once the specificity of this approach is documented with further research, it might be possible to use conservative, minimally invasive approaches in patients with low-grade DCIS, which would decrease the economic and social burden associated with breast cancer (44). Diffusion-weighted imaging could also potentially help decrease the distress of women in whom low-risk DCIS has been diagnosed because they would be offered lighter treatment options than those treated for invasive breast cancer (45).

**Acknowledgments:** The authors thank Akitoshi Takamine, RT, Kiyoshi Kosaka, RT, and Teruaki Nishida, RT, of Kitano Hospital, Osaka, Japan, for their excellent technical assistance and kind support.

**Disclosures of Potential Conflicts of Interest:** **M.I.** No potential conflicts of interest to disclose. **D.L.B.** No potential conflicts of interest to disclose. **R.O.** No potential conflicts of interest to disclose. **T.O.** No potential conflicts of interest to disclose. **K.F.** No potential conflicts of interest to disclose. **S.K.** No potential conflicts of interest to disclose. **S.T.** No potential conflicts of interest to disclose. **M.F.** No potential conflicts of interest to disclose. **H.S.** No potential conflicts of interest to disclose. **K.T.** No potential conflicts of interest to disclose.

## References

1. Ernster VL, Ballard-Barbash R, Barlow WE, et al. Detection of ductal carcinoma in situ in women undergoing screening mammography. J Natl Cancer Inst 2002;94(20):1546–1554.
2. Erbas B, Provenzano E, Armes J, Gertig D. The natural history of ductal carcinoma in situ of the breast: a review. Breast Cancer Res Treat 2006;97(2):135–144.
3. Sanders ME, Schuyler PA, Dupont WD, Page DL. The natural history of low-grade ductal carcinoma in situ of the breast in women treated by biopsy only revealed over 30 years of long-term follow-up. Cancer 2005;103(12):2481–2484.
4. Boecker W. Preneoplasia of the breast: a new conceptual approach to proliferative breast disease. Munich, Germany: Saunders Elsevier, 2006; 428.
5. Dinkel HP, Gassel AM, Tschammler A. Is the appearance of microcalcifications on mammography useful in predicting histological grade of malignancy in ductal cancer in situ? Br J Radiol 2000;73(873):938–944.
6. Kuhl C. The current status of breast MR imaging. I. Choice of technique, image interpretation, diagnostic accuracy, and transfer to clinical practice. Radiology 2007;244(2):356–378.
7. Berg WA, Gutierrez L, NessAiver MS, et al. Diagnostic accuracy of mammography, clinical examination, US, and MR imaging in preoperative assessment of breast cancer. Radiology 2004;233(3):830–849.
8. Neubauer H, Li M, Kuehne-Heid R, Schneider A, Kaiser WA. High grade and non–high grade ductal carcinoma in situ on dynamic MR mammography: characteristic findings for signal increase and morphological pattern of enhancement. Br J Radiol 2003;76(901):3–12.
9. Kuhl CK, Schrading S, Bieling HB, et al. MRI for diagnosis of pure ductal carcinoma in situ: a prospective observational study. Lancet 2007;370(9586):485–492.
10. Le Bihan D, Breton E, Lallemand D, Grenier P, Cabanis E, Laval-Jeantet M. MR imaging of intravoxel incoherent motions: application to diffusion and perfusion in neurologic disorders. Radiology 1986;161(2):401–407.
11. Le Bihan D. Molecular diffusion, tissue microdynamics and microstructure. NMR Biomed 1995;8(7-8):375–386.
12. Takahara T, Imai Y, Yamashita T, Yasuda S, Nasu S, Van Cauteren M. Diffusion-weighted whole body imaging with background body signal suppression (DWIBS): technical improvement using free breathing, STIR and high resolution 3D display. Radiat Med 2004;22(4):275–282.
13. Tamai K, Koyama T, Saga T, et al. The utility of diffusion-weighted MR imaging for differentiating uterine sarcomas from benign leiomyomas. Eur Radiol 2008;18(4):723–730.
14. Tamai K, Koyama T, Saga T, et al. Diffusion-weighted MR imaging of uterine endometrial cancer. J Magn Reson Imaging 2007;26(3):682–687.
15. Le Bihan D. The "wet mind": water and functional neuroimaging. Phys Med Biol 2007;52(7):R57–R90.
16. Kuroki-Suzuki S, Kuroki Y, Nasu K, Nawano S, Moriyama N, Okazaki M. Detecting breast cancer with non-contrast MR imaging: combining diffusion-weighted and STIR imaging. Magn Reson Med Sci 2007;6(1):21–27.
17. Guo Y, Cai YQ, Cai ZL, et al. Differentiation of clinically benign and malignant breast lesions using diffusion-weighted imaging. J Magn Reson Imaging 2002;16(2):172–178.
18. Woodhams R, Matsunaga K, Iwabuchi K, et al. Diffusion-weighted imaging of malignant breast tumors: the usefulness of apparent diffusion coefficient (ADC) value and ADC map for the detection of malignant breast tumors and evaluation of cancer extension. J Comput Assist Tomogr 2005;29(5):644–649.
19. Woodhams R, Matsunaga K, Kan S, et al. ADC mapping of benign and malignant breast tumors. Magn Reson Med Sci 2005;4(1):35–42.
20. Partridge SC, Demartini WB, Kurland BF, Eby PR, White SW, Lehman CD. Differential diagnosis of mammographically and clinically occult breast lesions on diffusion-weighted MRI. J Magn Reson Imaging 2010;31(3):562–570.

21. Silverstein M, Lagios M, Craig P, et al. The Van Nuys prognostic index for ductal carcinoma in situ. Breast J 1996;2(1):38–40.
22. Silverstein MJ, Lagios MD, Craig PH, et al. A prognostic index for ductal carcinoma in situ of the breast. Cancer 1996;77(11):2267–2274.
23. Bianchi S, Vezzosi V. Microinvasive carcinoma of the breast. Pathol Oncol Res 2008;14(2):105–111.
24. Jansen SA, Newstead GM, Abe H, Shimauchi A, Schmidt RA, Karczmar GS. Pure ductal carcinoma in situ: kinetic and morphologic MR characteristics compared with mammographic appearance and nuclear grade. Radiology 2007;245(3):684–691.
25. Tavassoli FA, Devilee P, eds. World Health Organization classification of tumours: pathology and genetics of tumours of the breast and female genital organs. Lyon, France: IARC Press, 2003.
26. SAS Institute. SAS/STAT user's guide, version 9.2. Cary, NC: SAS Institute, 2009.
27. Allegra CJ, Aberle DR, Ganschow P, et al. NIH state-of-the-science conference statement: diagnosis and management of ductal carcinoma in situ (DCIS). NIH Consens State Sci Statements 2009;26(2):1–27.
28. Silverstein MJ, Rosser RJ, Gierson ED, et al. Axillary lymph node dissection for intraductal breast carcinoma—is it indicated? Cancer 1987;59(10):1819–1824.
29. Baxter NN, Virnig BA, Durham SB, Tuttle TM. Trends in the treatment of ductal carcinoma in situ of the breast. J Natl Cancer Inst 2004;96(6):443–448.
30. Kitis O, Altay H, Calli C, Yunten N, Akalin T, Yurtseven T. Minimum apparent diffusion coefficients in the evaluation of brain tumors. Eur J Radiol 2005;55(3):393–400.
31. Sugahara T, Korogi Y, Kochi M, et al. Usefulness of diffusion-weighted MRI with echo-planar technique in the evaluation of cellularity in gliomas. J Magn Reson Imaging 1999;9(1):53–60.
32. Yoshikawa MI, Ohsumi S, Sugata S, et al. Relation between cancer cellularity and apparent diffusion coefficient values using diffusion-weighted magnetic resonance imaging in breast cancer. Radiat Med 2008;26(4):222–226.
33. Maffuz A, Barroso-Bravo S, Nájera I, Zarco G, Alvarado-Cabrero I, Rodríguez-Cuevas SA. Tumor size as predictor of microinvasion, invasion, and axillary metastasis in ductal carcinoma in situ. J Exp Clin Cancer Res 2006;25(2):223–227.
34. Partridge SC, Mullins CD, Kurland BF, et al. Apparent diffusion coefficient values for discriminating benign and malignant breast MRI lesions: effects of lesion type and size. AJR Am J Roentgenol 2010;194(6):1664–1673.
35. Doskaliyev A, Yamasaki F, Ohtaki M, et al. Lymphomas and glioblastomas: differences in the apparent diffusion coefficient evaluated with high *b*-value diffusion-weighted magnetic resonance imaging at 3T. Eur J Radiol 2010. doi:10.1016/j.ejrad.2010.11.005. Published December 1, 2010.
36. Vlastos G, Verkooijen HM. Minimally invasive approaches for diagnosis and treatment of early-stage breast cancer. Oncologist 2007;12(1):1–10.
37. Kettritz U. Modern concepts of ductal carcinoma in situ (DCIS) and its diagnosis through percutaneous biopsy. Eur Radiol 2008;18(2):343–350.
38. Yabuuchi H, Matsuo Y, Okafuji T, et al. Enhanced mass on contrast-enhanced breast MR imaging: lesion characterization using combination of dynamic contrast-enhanced and diffusion-weighted MR images. J Magn Reson Imaging 2008;28(5):1157–1165.
39. Woodhams R, Kakita S, Hata H, et al. Identification of residual breast carcinoma following neoadjuvant chemotherapy: diffusion-weighted imaging—comparison with contrast-enhanced MR imaging and pathologic findings. Radiology 2010;254(2):357–366.
40. Bogner W, Gruber S, Pinker K, et al. Diffusion-weighted MR for differentiation of breast lesions at 3.0 T: how does selection of diffusion protocols affect diagnosis? Radiology 2009;253(2):341–351.
41. Kriege M, Brekelmans CT, Boetes C, et al. Efficacy of MRI and mammography for breast cancer screening in women with a familial or genetic predisposition. N Engl J Med 2004;351(5):427–437.
42. Gill JK, Maskarinec G, Pagano I, Kolonel LN. The association of mammographic density with ductal carcinoma in situ of the breast: the Multiethnic Cohort. Breast Cancer Res 2006;8(3):R30.
43. Park MJ, Cha ES, Kang BJ, Ihn YK, Baik JH. The role of diffusion-weighted imaging and the apparent diffusion coefficient (ADC) values for breast tumors. Korean J Radiol 2007;8(5):390–396.
44. Pediconi F, Padula S, Dominelli V, et al. Role of breast MR imaging for predicting malignancy of histologically borderline lesions diagnosed at core needle biopsy: prospective evaluation. Radiology 2010;257(3):653–661.
45. Kennedy F, Harcourt D, Rumsey N, White P. The psychosocial impact of ductal carcinoma in situ (DCIS): a longitudinal prospective study. Breast 2010;19(5):382–387.